



Magnetizing Characteristics of a Flux-Coupling Type Superconducting Fault Current Limiter Connected in Parallel between Two Coils Using an E–I Iron Core

Seok-Cheol Ko² · Tae-Hee Han³ · Sung-Hun Lim¹

Received: 18 November 2018 / Revised: 30 January 2019 / Accepted: 11 February 2019 / Published online: 25 February 2019
© The Korean Institute of Electrical Engineers 2019

Abstract

In power systems, there are short-circuit faults due to various causes. One way to reduce this fault current is the superconducting fault current limiter (SFCL). Since the current limiter model using a winding includes an iron core, the magnetizing current generated in the iron core when the fault current is limited should not be as large as possible. That is, when saturation of the iron core occurs, sufficient magnetic flux is not generated and the fault current limiting characteristics are degraded. Therefore, in this paper, a flux-coupling type SFCL using an E–I iron core was fabricated to effectively reduce the saturation of the iron core and limit the fault current to twice. The two major windings N_1 and N_2 were connected in parallel, and the peak current limiting characteristics and voltage waveforms were compared based on the winding directions of the two coils. The two main coils were also connected in parallel to analyze the flux linkage and instantaneous power characteristics. The magnetization power area and operating range of the flux linkage based on the magnetic flux energy accumulated in the E–I iron core were compared and analyzed in relation to the increase or decrease of the magnetizing current.

Keywords Flux-coupling type · Superconducting fault current limiter (SFCL) · Magnetizing current · Magnetizing power area · Flux linkage and instantaneous power characteristics

1 Introduction

Short circuit accidents in power systems occur frequently from various causes. A representative system with the functionality to prevent such accidents is the superconducting fault current limiter (SFCL) [1]. The SFCL is considered the most ideal device for limiting the short circuit level caused by an impedance close to zero in a normal state and a fast

transition to a steady-state. To date, various types of SFCL have been developed including resistive, saturated iron-core, magnetic shielding, bridge, active and high speed switching, inductive and hybrid, transformer, flux-coupling and flux-lock [2–7].

Recently, research on the structure and application of the flux-coupling type SFCL has been carried out all over the world. The flux-coupling type SFCL easily controls the current limiting impedance ratio and has a low steady-state impedance that aids the system reclosing [8–11]. Development of various types of SFCLs has been accelerated in attempts to reduce the powder burden of the high temperature superconducting (HTSC) element in the SFCL [12–14].

In previous studies, the research team of this paper proposed an SFCL structure where the two main windings were connected in series or in parallel using two iron cores [15–17]. The HTSC element was added to the structure by including a tertiary winding to another iron core. Additional research results were reported on the double peak current limiting operation and recovery characteristics, and magnetization characteristics according to the fault angle during fault occurrence [18]. Since the current limiting model

✉ Sung-Hun Lim
superlsh73@ssu.ac.kr

Seok-Cheol Ko
suntrac@kongju.ac.kr

Tae-Hee Han
hantaehae@jwu.ac.kr

¹ Department of Electrical Engineering, Soongsil University, Seoul, South Korea

² Industry-University Cooperation Foundation, Kongju National University, Gongju, South Korea

³ Department of Aero Materials Engineering, Jungwon University, Goesan, South Korea

includes an iron core, the magnetizing current generated from the iron core should not be as large as possible when limiting the fault current. If saturation occurs, sufficient magnetic flux does not occur and the fault current limiting characteristics are reduced.

Therefore, in this paper, we tried to analyze the magnetization characteristics, which are the saturation characteristics of the iron core in the test of the fault current limiting operation. A flux-coupling type SFCL with two magnetic flux paths was fabricated to effectively reduce the saturation of the iron core and limit the fault current to twice. The magnetizing current (I_m) and limit impedance (Z_{SFCL}) equations for the flux-coupling type SFCL connected in parallel were derived from the electrical magnetic field equivalent circuit. Short circuit experiments were carried out to compare the double peak current limiting operation and the voltage waveforms of each element before and after the fault occurrence. The waveforms of these experimental results were used with the ORIGIN PRO 8 program. Moreover, the flux linkages and instantaneous power characteristics were analyzed depending on the winding direction of the main coils. The magnetizing power area and variation of flux linkage's operating range were comparatively analyzed according to the increase or decrease of the magnetizing current during the fault occurrence period.

2 Structure and Operation Principle

2.1 Structure and Principle

As shown in Fig. 1, the flux-coupling type SFCL is composed of an E–I iron core, three windings, and two HTSC elements. The two main coils N_1 and N_2 are connected in parallel, and the secondary winding (N_2) and HTSC element 1 (R_{SC1}) are connected in series. Also, a tertiary coil (N_3) was added to the third leg of the E–I iron core to connect in series HTSC element 2 (R_{SC2}).

The basic operating principle of the flux-coupling type SFCL is as follows. Under normal operation, the magnetic fluxes coming out of the coils between N_1 and N_2 are canceled

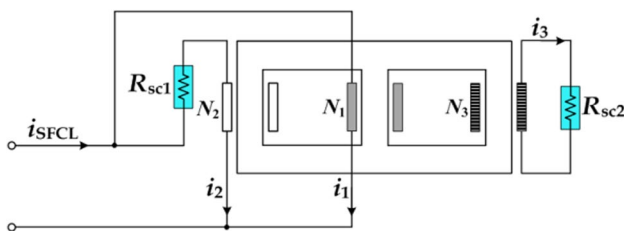


Fig. 1 Schematic configuration of flux-coupling type SFCL connected in parallel with two flux paths using an E–I iron core

out so that no magnetic fluxes from the N_3 coil are generated. If the coil resistance and magnetic flux leakage within the iron core are ignored, the voltage induced from all three coils almost remains at zero. However, during a fault occurrence, the quenching of the HTSC element 1 connected to the second coil leads to the generation of magnetic flux between the two coils due to the transient fault current. This induces a magnetic flux in the tertiary coil as well, resulting in limiting of the fault current by the flux-coupling type SFCL. Because a large fault current induces greater magnetic fluxes in the secondary and tertiary coils, the larger voltage across the secondary coil as well as the tertiary coil results in the quenching of the second HTSC element 2, which is connected to the tertiary coil. This contributes to the double peak limiting operation, which limits the second fault current.

2.2 Equivalent Circuit

Figure 2 shows the electrical equivalent circuit of a flux-coupling type SFCL with two magnetic flux paths using an E–I iron core. The electrical equivalent circuit can be derived from the magnetic equivalent circuit using the duality method [18]. The resistance and leakage inductance of each winding have been omitted for convenient analysis. L_1 and L_{Th} refer to the self-inductance of the winding about the center leg of the E–I iron core and the equivalent inductance of the two windings about the left and right legs of the iron core, respectively.

The magnetizing current (I_m) and limit impedance (Z_{SFCL}) of the flux-coupling type SFCL with the primary and secondary windings connected in parallel can be expressed as Eqs. (1) and (2), respectively.

$$I_m = I_1 - \left(\frac{N_2}{2N_1} I_2 + \frac{N_3}{2N_1} I_3 \right) \tag{1}$$

$$Z_{SFCL} = 1 / \left[\frac{1}{V_1} \left(\frac{N_2}{2N_1} \frac{V_{SC1}}{R_{SC1}} + \frac{N_3}{2N_1} \frac{V_{SC2}}{R_{SC2}} \right) + \frac{1}{j\omega L_{eq}} \right] \tag{2}$$

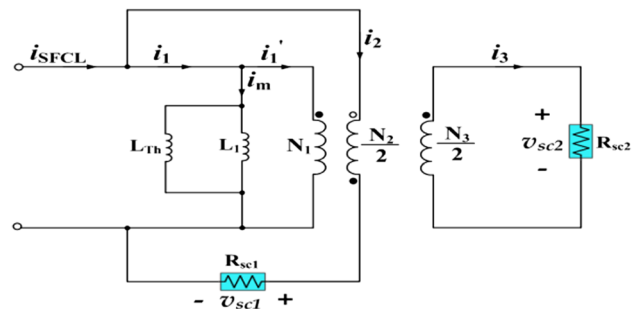


Fig. 2 Electrical equivalent circuit of flux-coupling type SFCL connected in parallel with two flux paths using an E–I iron core

Here, I_m was calculated from the current actually flowing in the three coils. V_1 , V_2 , V_{SC1} and V_{SC2} expressed in phasor form refer to the induced voltages for the primary coil, secondary coil, HTSC elements 1 and 2, respectively. N_1 , N_2 , and N_3 refer to the winding number for each winding, and L_{eq} is equal to L_{Th}/L_1 . R_{SC1} and R_{SC2} refer to the resistance of HTSC elements 1 and 2, respectively, and ω is the angular frequency. I_2 and I_3 of Eq. (1) showing the magnetizing current derived from the equivalent circuit in Fig. 2 refer to the current flowing in the secondary and tertiary coils, respectively.

3 Experimental Results and Discussion

3.1 Experimental Preparation

Experiments are performed to verify the fault current limiting operation of the flux-coupling type SFCL. As shown in Fig. 3, the experimental setup consists of a 60 Hz AC power supply (E_{in}), 0.66Ω line reactance (X_{line}), 0.096Ω line resistance (R_{line}), 51.5Ω load resistance (R_{load}), three windings, E–I core, HTSC elements, and fault generator. Key experimental parameters are listed in Table 1.

HTSC elements are immersed in 77 K liquid nitrogen. The $Y_1Ba_2Cu_3O_{7-x}$ (YBCO) thin films used in HTSC elements were made from materials manufactured by THEVA, Germany. YBCO thin film of $0.3 \mu\text{m}$ was deposited on sapphire substrate with its diameter of 2 inch and a $0.2 \mu\text{m}$ thick gold layer was covered on it for bypass against hot spots. The HTSC element was fabricated by etching the YBCO thin film into 2 mm wide and 420 mm long meander line using photolithography technique which consisted of fourteen stripes with different length, respectively [14]. The critical temperature and critical current of the HTSC elements are 87 K and 27 A, respectively.

SW_1 and SW_2 are thyristor switches controlled by a switch controller. It was designed so that after SW_1 is closed, SW_2 is closed at a fault angle of 0° of the AC power supply

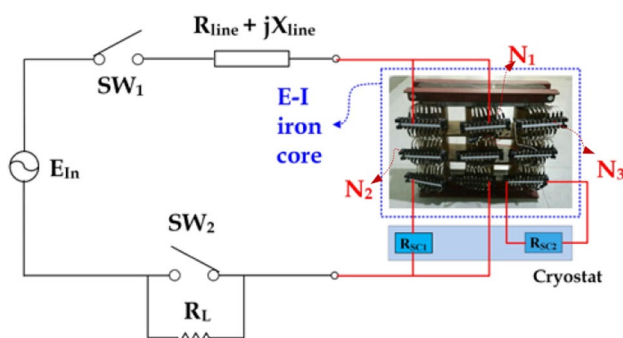


Fig. 3 The experimental test circuit

Table 1 Specifications of flux-coupling type SFCL connected in parallel with two flux paths using an E–I iron core

	Value	Unit
Iron core		
Left and right leg mean length (l_2, l_3)	580	mm
Center leg mean length (l_1)	310	mm
Cross sectional area (S_{core})	2790	mm ²
Two coils		
Turn number of primary winding (N_1)	45	Turns
Turn number of secondary winding (N_2)	15	Turns
Turn number of tertiary winding (N_3)	30	Turns
HTSC element		
Material	YBCO	–
Fabrication form	Thin Film	–
Critical temperature	87	K
Critical current	27	A

and then reopened after 5 cycles. The sampling precision was set to $50 \mu\text{s}$ to ensure the accuracy and completeness of the waveforms. The total time of the experiment data collection is 1000 ms.

The peak fault current limiting operation and magnetization characteristics occurring in the flux-coupling type SFCL due to the transient fault current were investigated using the induced voltages of the three coils and two HTSC elements. The magnetic flux linkage (λ) of the magnetization branch was obtained by integrating the voltage induced from the primary coil of the central leg of the E–I iron core.

3.2 Results and Discussions

Figure 4 shows the peak fault current limiting characteristics and voltage waveforms of each winding and element before and after fault occurrence for the flux-coupling type SFCL, with the primary and secondary windings in subtractive polarity winding and connected in parallel.

As shown in Fig. 4a, as the transient fault current (i_{SFCL}) increases, the current flowing in the secondary winding (i_2) exceeds the first critical current and the current flowing in the tertiary winding (i_3) also exceeds the second critical current (i_c). This result shows that the HTSC element 2 voltage (V_{SC2}) is induced after the HTSC element 1 voltage (V_{SC1}) is first occurred. HTSC elements 1 and 2 are being quenched consecutively.

Figure 4b shows that voltage is induced in the primary, secondary, and tertiary coils, since the magnetic fluxes occurred in the main windings of the primary and secondary coils did not cancel out simultaneously with the fault occurrence.

Figure 5 shows the peak fault current limiting characteristics and voltage waveforms of each winding and element

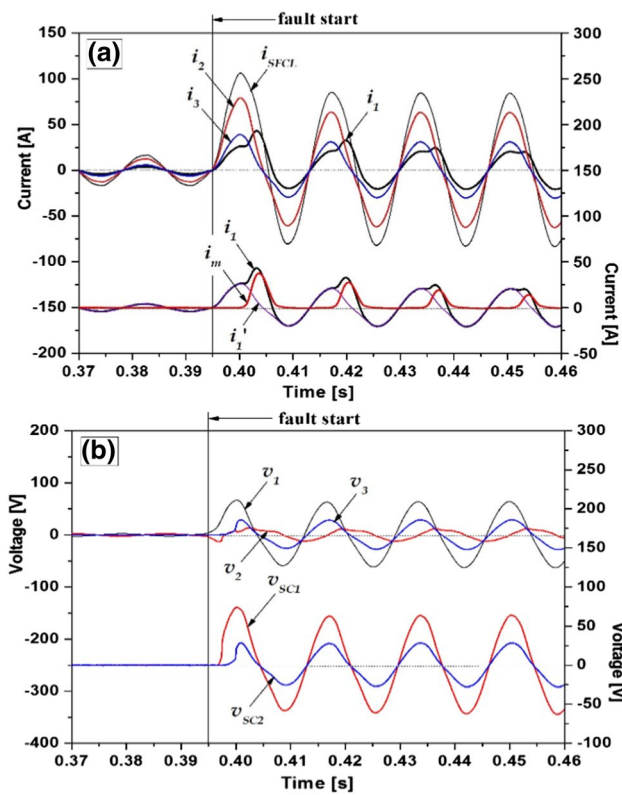


Fig. 4 Peak current limiting characteristics and voltage waveforms of a flux-coupling type SFCL connected in parallel with two flux paths when its two coils are designed with a subtractive polarity winding. **a** Current waveforms of SFCL and each winding including magnetization current (i_{SFCL} , i_1 , i_2 , i_3 , and i_m). **b** Voltage waveforms of each winding and each HTSC element (V_1 , V_2 , V_3 , V_{SC1} , and V_{SC2})

before and after fault occurrence, for the flux-coupling type SFCL with the primary and secondary windings in additive polarity winding and connected in parallel.

As shown in Fig. 5a, when the fault occurs for a small transient fault current (i_{SFCL}), the current flowing in the tertiary winding (i_3) did not exceed the critical current (i_C) after the current flowing in the secondary winding (i_2) exceeded the first critical current. As a result, the quench only occurred in HTSC element 1, while quench did not occur in HTSC element 2.

Figure 5b shows that the magnetic fluxes produced in the primary and secondary windings did not cancel out, so that voltage was induced only in the primary and secondary coils, and no voltage was induced in the tertiary coil. Since the winding directions of the primary and secondary coils are additive polarity winding, a significantly large voltage is induced in the primary coil compared to the subtractive polarity winding case. Since the critical current is not exceeded in HTSC element 2, the voltage induced in the tertiary coil can be observed to be zero.

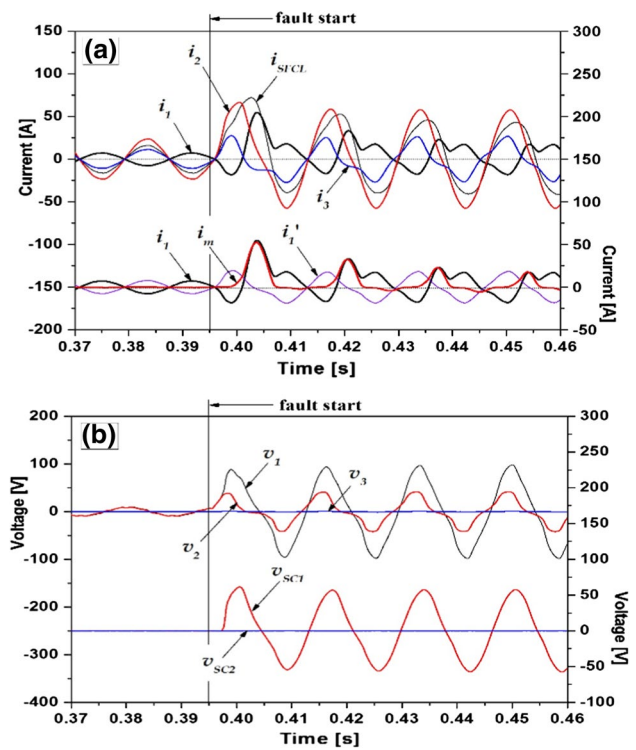


Fig. 5 Peak current limiting characteristics and voltage waveforms of a flux-coupling type SFCL connected in parallel with two flux paths when its two coils are designed with an additive polarity winding. **a** Current waveforms of SFCL and each winding including magnetization current (i_{SFCL} , i_1 , i_2 , i_3 , and i_m). **b** Voltage waveforms of each winding and each HTSC element (V_1 , V_2 , V_3 , V_{SC1} , and V_{SC2})

Figure 6 shows the flux linkage of each winding (λ) and the instantaneous power (P) burden characteristics of each element for the flux-coupling type SFCL, according to the winding directions of the two main windings or the primary and secondary coils. The flux linkage of the primary winding (λ_1) was more than twice higher when connected in additive polarity winding, compared to the subtractive polarity winding. On the other hand, the instantaneous power consumed by the SFCL and each element was observed to be significantly greater when the primary and secondary windings were connected with a subtractive polarity winding compared to the additive polarity winding.

As shown in Fig. 6a, the power consumption of the SFCL (p_{SFCL}) was highest, followed by the power consumption of HTSC element 1 (p_{SC1}), HTSC element 2 (p_{SC2}), and the magnetizing power (p_m) for the instantaneous power burden of the subtractive polarity winding.

As shown in Fig. 6b, the power consumption of the SFCL (p_{SFCL}) was highest followed by the power consumption of HTSC element 1 (p_{SC1}), magnetizing power (p_m), and HTSC element 2 (p_{SC2}) for the instantaneous power burden of the additive polarity winding.

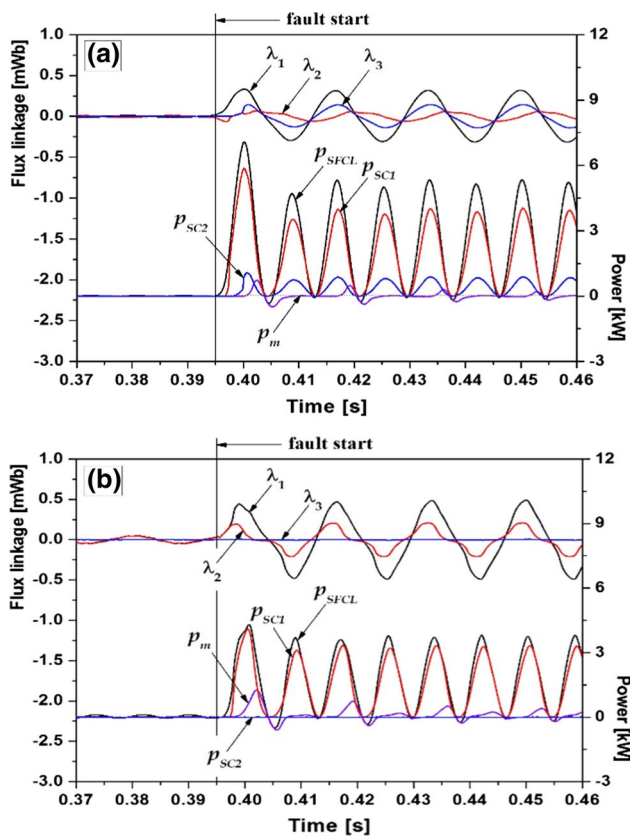


Fig. 6 Flux linkages (λ) and instantaneous power (P) characteristics of a flux-coupling SFCL with two flux paths, depending on the winding direction between two coils: **a** subtractive polarity winding, **b** additive polarity winding

Figure 7 shows a plot comparing the variation in magnetizing power area based on increasing magnetizing current when the winding directions between the primary and secondary coils were a subtractive polarity winding, and an additive polarity winding, respectively.

Figure 7a shows the change in magnetizing power obtained by multiplying the magnetizing current and magnetization branch voltage for the subtractive polarity winding of the primary and secondary coils, and fault periods 1–4. This allows analysis of the accumulated magnetic energy of the E–I iron core.

Figure 7b shows the change in magnetizing power for the case with additive polarity winding for the primary and secondary coils. Comparison of variation in the magnetizing power based on the winding direction revealed that the change in magnetizing power is significantly larger for the additive polarity winding case than the subtractive polarity winding case.

Figure 8 shows a comparison curve of the flux linkage (λ) operating range for the additive and subtractive polarity winding directions for the primary and secondary coils, for increasing magnetizing current. The flux linkage induced in

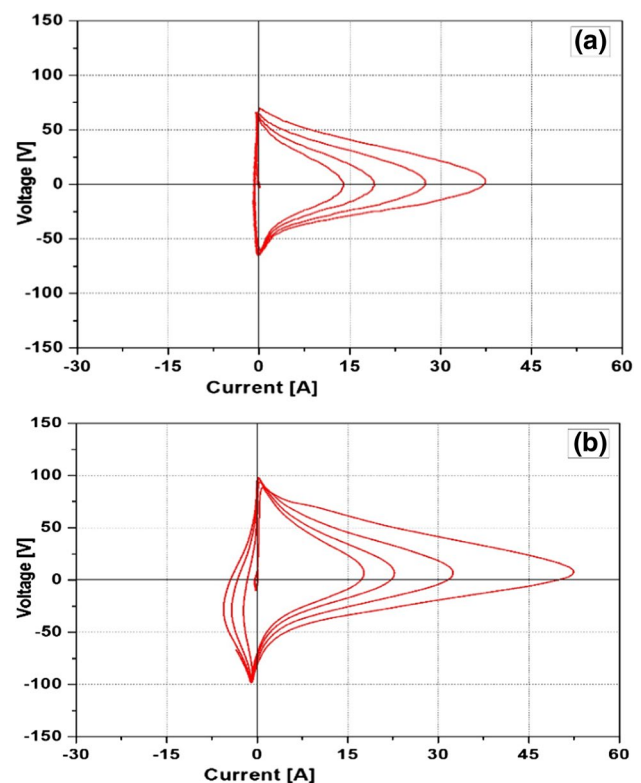


Fig. 7 Variation in magnetizing power (p_m) area dependent on the magnetization current (i_m) as the fault period passes, after a fault occurrence in the flux-coupling type SFCL with two flux paths: **a** subtractive polarity winding, **b** additive polarity winding

the magnetization branch can be determined by integrating the voltage induced in the primary winding of the SFCL.

Progressing from fault period 1–4, it can be observed that the flux linkage operating range decreased along with the decreasing magnetizing current. In particular, comparison of the subtractive polarity winding and additive polarity winding cases for the two coils reveals there was a greater decrease in the flux linkage operating range with the decrease in magnetizing current for the additive polarity winding, versus the subtractive polarity winding. There is a larger increase in magnetizing current because of the large transient fault current, and because of this, it can be predicted that the larger magnetic field energy is accumulated in the E–I iron core.

4 Conclusion

In this study, the magnetization characteristics of a flux-coupling type SFCL with two magnetic flux paths were analyzed, considering peak fault current limiting performance for a large initial transient fault current, and saturation prevention of the iron core. An electrical equivalent circuit with

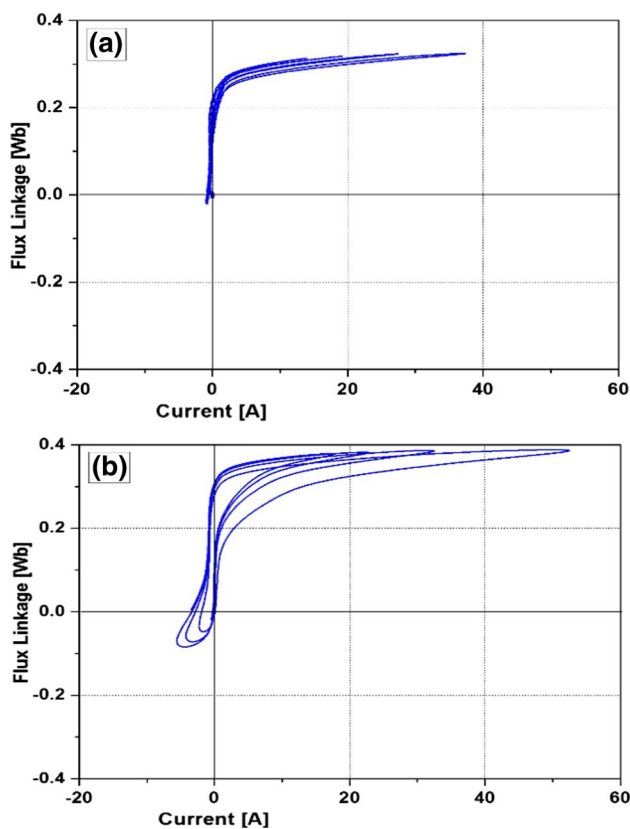


Fig. 8 Flux linkage (λ) operating range depending on the magnetization current (i_m) as the fault period passes after the fault occurs in a flux-coupling type SFCL with two flux paths: **a** subtractive polarity winding, **b** additive polarity winding

a magnetization branch was created to analyze the magnetization characteristics and double peak fault current limiting operation of the SFCL. The magnetizing current and limit impedance equations were derived. Compared to the subtractive polarity winding case, when the winding directions of the main windings or primary and secondary coils were additive polarity winding, a significantly large voltage was induced in the primary coil, along with quenching of HTSC element 1. No quench occurred in HTSC element 2. Also, the flux linkage (λ) of the primary winding was more than two times greater for the additive polarity winding compared to the subtractive polarity winding.

On the other hand, the instantaneous power consumed by the SFCL and each device were found to be considerably greater for the subtractive polarity winding case compared to the additive polarity winding case. Comparison of the variation in magnetizing power based on the winding direction using calculations of the measured voltage and current values revealed that the variation in magnetizing power was significantly greater for the additive polarity winding compared to the subtractive polarity winding. Furthermore, it was observed that there was a greater decrease in the flux

linkage operating range for the additive polarity winding than the subtractive polarity winding.

Acknowledgements This work was supported by the research grant of the Kongju National University in 2018.

References

- Hara T, Okuma T, Yamamoto T, Ito D, Tasaki K, Tsurunaga K (1993) Development of a new 6.6 kV/1500 A class superconducting fault current limiter for electric power systems. *IEEE Trans Power Deliv* 8(1):182–192
- Noe M, Steurer M (2007) High-temperature superconductor fault current limiters: concepts, applications, and development status. *Supercond Sci Technol* 20(3):R15–R29
- Neumueller HW et al (2009) Development of resistive fault current limiters based on YBCO coated conductors. *IEEE Trans Appl Supercond* 19(3):1950–1955
- Salim KM, Hoshino T, Kawasaki A, Muta I, Nakamura T (2003) Waveform analysis of the bridge type SFCL during load changing and fault time. *IEEE Trans Appl Supercond* 13(2):1992–1995
- Hekmati A (2015) Multiobjective design of tunable shield-type superconducting fault current limiter. *IEEE Trans Appl Supercond* 25(5):5602908
- Choi HS, Lim SH (2007) Operating performance of the flux-lock and the transformer type superconducting fault current limiter using the YBCO thin films. *IEEE Trans Appl Supercond* 17(2):1823–1826
- Xin Y et al (2012) Development of a 220 kV/300 MVA superconductive fault current limiter. *Supercond Sci Technol* 25(10):105011
- Ren L et al (2010) Techno-economic evaluation of a novel flux-coupling type superconducting fault current limiter. *IEEE Trans Appl Supercond* 20(3):1242–1245
- Chen L, Tang YJ, Li Z, Shi J, Cheng SJ (2010) Current limiting characteristics of a novel flux-coupling type superconducting fault current limiter. *IEEE Trans Appl Supercond* 20(3):1143–1146
- Deng CH et al (2015) Study of a modified flux-coupling-type superconducting fault current limiter for mitigating the effect of DC short circuit in a VSC-HVDC system. *J Supercond Novel Magn* 28(5):1525–1534
- Lee GH et al (2009) Hybrid superconducting fault current limiter of the first half cycle non-limiting type. *IEEE Trans Appl Supercond* 19(3):1888–1891
- Kim JS, Lim SH, Kim JC (2012) Comparative analysis on current limiting characteristics of hybrid superconducting fault current limiters (SFCLs) with first half cycle limiting and non-limiting operations. *J Electr Eng Technol* 7(5):659–663
- Zhao Y, Saha TK, Krause O, Li Y (2016) Current limiting impedance comparison between different designs of iron cores of the flux-lock-type superconducting fault current limiter. *IET Gener Transmiss Distrib* 10(2):548–554
- Lim SH, Moon JF, Kim JC (2009) Improvement on current limiting characteristics of a flux-lock type SFCL using E–I core. *IEEE Trans Appl Supercond* 19(3):1904–1907
- Ko S, Lim SH, Han TH (2013) Analysis on fault current limiting and recovery characteristics of a flux-lock type SFCL with an isolated transformer. *Physica C* 484:263–266
- Ko SC, Han TH, Lim SH (2014) Analysis on current limiting characteristics according to the influence of the magnetic flux for SFCL with two magnetic paths. *J Electr Eng Technol* 9(6):1909–1913

17. Lim SH, Kim YP, Ko SC (2016) Effect of peak current limiting in series-connection SFCL with two magnetically coupled circuits using E-I core. *IEEE Trans Appl Supercond* 26(3):5600404
18. Ko SC, Lim SH (2016) Analysis on magnetizing characteristics due to peak fault current limiting operation of a modified flux-lock-type SFCL with two magnetic paths. *IEEE Trans Appl Supercond* 26(4):5601605

Publisher's Note Springer Nature remains neutral with regard to jurisdictional claims in published maps and institutional affiliations.



Seok-Cheol Ko received his B.S., M.S., and Ph.D. degrees from Chonbuk National Univ., Korea in 1996, 2002, and 2005, respectively. Currently, he is a professor in the Industry-University Cooperation Foundation at Kongju National Univ., Kongju, Korea.



Sung-Hun Lim received his B.S., M.S., and Ph.D. degrees from Chonbuk National Univ., Korea in 1996, 1998, and 2003, respectively. Currently, he is a professor in the Dept. of Electrical Engineering at Soongsil Univ., Seoul, Korea.



Tae-Hee Han received his B.S., M.S., and Ph.D. degrees from Chonbuk National Univ., Korea in 1991, 1994, and 1999, respectively. Currently, he is a professor in the Dept. of Aero Materials Engineering at Jungwon Univ., Goesan, Korea.